KfK 2986
September 1980

Friction and Heat Transfer Correlations for the Roughness of the BR2-Calibration Element

L. Meyer
Institut für Neutronenphysik und Reaktortechnik
Projekt Schneller Brüter

Kernforschungszentrum Karlsruhe

KERNFORSCHUNGSZENTRUM KARLSRUHE
Institut für Neutronenphysik und Reaktortechnik
Projekt Schneller Brüter

KfK 2986

Friction and Heat Transfer Correlations for the Roughness of the BR2 - Calibration Element

L. Meyer

Kernforschungszentrum Karlsruhe GmbH, Karlsruhe

Kernforschungszentrum Karlsruhe GmbH
ISSN 0303-4003

Abstract

Heat transfer and pressure drop measurements at a single rough rod in a smooth tube were performed with air and evaluated by a method developed in the INR. Friction factors, Stanton numbers and R- and G-functions are reported.

Reibungskoeffizienten und Wärmeübergangskorrelationen für die Rauhigkeit des BR2 - Kalibrierelementes

Zusammenfassung

An einem rauhen Einzelstab in einem glatten Rohr wurden Wärmeübergangs- und Druckverlustmessungen mit Luft durchgeführt und mit einer Methode, die im INR entwickelt wurde, ausgewertet. Es werden Reibungskoeffizienten, Stanton-Zahlen und R- und G-Funktionen angegeben.

1. Introduction

In the past years experiments were performed with bundles of 12 rods in order to get information relevant to the thermohydraulic design of the rod clusters under irradiation in the BR2 /1,2/. These rods had artificial roughness with transverse trapezoidal ribs and were heated electrically and cooled by helium. The experimental results were used for comparison with results computed by the SAGAPO-code /1,2/. For these calculations correlations for the roughness parameters of the laws of the wall for the velocity and temperature distribution were used, which were obtained from a preliminary test of a single rod in a large outer shroud and from tests at sharp edged rectangular ribs /3/. Some information came also from a test of a single rod with a similar roughness geometry, however, for reliable heat transfer results this rod was instrumented with too few thermocouples /4/. Isothermal tests at similar roughnesses to investigate the velocity distribution were performed in a rectangular channel /5/ and in a wall subchannel of a rod bundle /6/.

The present experiment was conducted with a single BR2 rod in a smooth outer shroud of 16 mm I.D. The results of the experiment are presented in terms of friction factors and Stanton numbers, both, for the entire annulus and transformed to the rough boundary condition, and in terms of the roughness parameters of nondimensional velocity and temperature distribution. The method used to transform the bulk data to the rough boundary condition is based on the 'laws of the wall'. Two 'laws of the wall' for the velocity profiles starting from both walls of the annlus are assumed and the intersection of the profiles is interpreted as the zero shear position /3/. The heat flux and thereby the temperature profile is transformed in such a way that there is no heat transfer across the surface of no shear /7/.

2. The experimental setup

The test rod consisted of a tube of stainless steel (1.4981) with 8.0 mm o.d. and a heated length of 684 mm. The volumetric diameter was 7.86 mm. The roughness geometry is shown in figure 1. For comparison the roughness geometries of the other investigations /4,5,6/ are shown in figures 2,3, and 4. The arrangement of the test rod in the outer smooth tube is shown in figure 5. The rod was heated electrically by alternating current.

Air is circulated by means of a compressor. The flow oscillations caused by the compressor are dampened by a large vessel. The air is subsequently depurated by the vapor content in a drier and goes to one of various orifice plates for the measurement of the mass flow. These orifice plates are placed in parallel and have been calibrated in the laboratory for the optimum application range. The air flows then through the annular test section, and finally to the atmosphere. By means of a valve placed downstream the test section it is possible to apply a certain back pressure, to increase the air density and therefore the maximum obtainable Reynolds number in the test section. The main characteristics of the air loop are the following:

Coolant max. pressure:	5 bar
Coolant outlet temperature:	20 ÷ 250°C
Coolant flow:	0.6 ÷ 90 g/sec
Heating power during experiments:	0 ÷ 13 KW
Rough rod wall temperature:	20 ÷ 400°C

The experimental apparatus was found to give good results in a test with a smooth tube /8/.

3. Evaluation

The experimental data were punched on tape and were evaluated with the computer code AURIS. The main features of this code are described in /3/. The latest changes and extensions regarding the Stanton number transformation and temperature effect reduction are described in /7/.

The measured temperatures of the heated rods were corrected for the thermocouple position, which was below the rough surface. With the rough rods being in fact a tube with an outer rough surface, it was assumed that the thermocouple junction was at the center of the tube wall.

The correction which takes account of the heat conduction in radial direction

$$T_W = T_{WM} - \frac{q\Delta r}{k_c 2} \tag{1}$$

was applied, with the thermal conductivity of the canning

$$k_c = 7.805 + 0.015823\ T \tag{2}$$

and Δr the thickness of the tube wall.
The maximum correction was 7K at the highest heat flux.
The so-called "fin efficiency effect" of rough surfaces /9/ was taken into account by

$$T_{WC} = (T_W - T_B) k_\infty + T_B \tag{3}$$

with

$$k_\infty = 1 - 0.4Bi \tag{4}$$

and

$$Bi = \frac{q\ h}{(T_W - T_B) k_c} \tag{5}$$

Here the maximum correction was 1.3 K.

The heat transfer by radiation was calculated with an emissivity coefficient of $\varepsilon_{12} = 0.341$.

The evaluation of friction and heat transfer coefficients and the transformation procedure was performed with local data along the test rod. Mean values were evaluated from local results in the section $23 \leq x/D_h \leq 45$. These mean values only are given in this report.

4. Results and discussion

The basic results, which are the bulk values of the Reynolds number the friction factor and the Stanton number and the transformed data were evaluated using the 'law of the wall' with a slope of $A_r = 2.5$. Since it was found for similar roughnesses in a parallel plate channel /5/ that the slope A_r should be lower and that it is a function of the ratio $h/\hat{y}$, the transformation was performed also with $A_r=1.7$. This value was found for $h/\hat{y} = 0.05$ and a volumetric definition of the hydraulic diameter /5/. Plots of these results are only shown if they differ significantly from the transformation with $A_r=2.5$. The results given in the tables were evaluated with $A_r \approx 2.5$.

4.1 Friction factors

Figure 6 (A) shows a plot of the bulk friction factors versus the Reynolds numbers. For comparison a line is shown, which represents the isothermal results from a rough rod with a similar roughness measured in the same outer shroud with air /4/. Although this roughness was not exactly the same as the present one, the isothermal friction factors are identical. There is a decrease of the friction factor with higher ratios of T_W/T_B, which is strongest in the range $10^4 < Re < 10^5$. This was found also in /4/.

The transformed friction factor f_1 pertaining to the rough zone only is shown in figure 6 (B). To reduce the temperature effect, which is more pronounced in f_1 than in f, the reduction found by Meyer and Rehme /7/ was applied

$$f_{1R} = f_1 \left(\frac{T_W}{T_1}\right)^{0.29} \tag{6}$$

The reduced friction factor f_{1R} is plotted versus Re_{1W} in figure 6 (C). The reduction is very good for low T_W/T_B-ratios but fails for high T_W/T_B-ratios and high Reynolds numbers, since there the temperature effect was practically zero. With the exception of these points the friction factor is constant, $f_{1R}=0.0176$ for $Re_{1W} > 4 \cdot 10^4$.

The results of the transformation with $A_r=1.7$ are not shown, because the differences are small. At $Re_1=5 \cdot 10^5$ the friction factor f_1 is lower by 1%. This difference increases up to 2.5% at $Re_1=10^4$ and is 3.3% at $Re_1=3 \cdot 10^3$.

4.2 Stanton numbers

Figure 7 (A) shows the Stanton numbers reduced for the Prandtl number effect ($St\ Pr^{0.6}$) versus the Reynolds numbers. With an increasing temperature ratio T_W/T_B the Stanton numbers decrease. Similar to the temperature effect on the friction factor this effect is lower at high Reynolds numbers. Therefore the temperature reduction of the form

$$St_R = St \left(\frac{T_W}{T_B}\right)^{0.25} \tag{7}$$

as it was found in /7/, is good for $Re > 10^5$, but is too low for lower Reynolds numbers. If the reduction formula is applied, which was developed in /7/,

$$St_R = \frac{St}{1+14Re^{-0.35} \lg\left[4.35 \left(\frac{x}{D_h}\right)^{-.6}\right]} \left(\frac{T_W}{T_B}\right)^{-ex} \tag{8}$$

with $$ex = -0.243 - \phi\left(\frac{x}{D_h}\right)\ 0.7\ \lg\left(\frac{T_W}{T_B}\right) \qquad (9)$$

and $$\phi\left(\frac{x}{D_h}\right) = 0.4\ \left(1 + \frac{x/D_h}{25}\right) \qquad (10)$$

the reduction is too high at high Reynolds numbers (Fig.7(B)). For comparison with the results from /4/ straight lines representing the reduced Stanton numbers found for the various gases are shown in figure 7(B). The exponents used in the temperature reduction equation (7) were however different. For air and nitrogen it was x=0.2, while for helium it was x=0.368.

Figure 8(A) shows the Stanton numbers transformed to the rough boundary conditions as it is described in /7/. The transformed Stanton number in the range $Re > 2 \cdot 10^4$ can be expressed as

$$St_T = 0.0165\ Re_1^{-0.11} Pr^{-0.6} \left(\frac{T_W}{T_1}\right)^{ex} XL \qquad (11)$$

with $$XL = 1 + 14 Re_1^{-0.35}\ \lg\left[4.35\ \left(\frac{x}{D_{h1}}\right)^{-.6}\right] \geq 1 \qquad (12)$$

The exponent ex is calculated by equation (9) with D_{h1} and T_1. For an exact correlation a Reynolds number dependent exponent is needed.

The results for a transformation with $A_r = 1.7$ are shown in figure 8 (B) together with the line according to equation (11). They are lower by 6% at high Reynolds numbers and by 13% at low Reynolds numbers.

The Stanton number transformed by a method developed by Firth /10/ is shown in Fig.8(C). The results are correlated by

$$St_T = 0.04263\ Pr^{-0.6}\ Re_1^{-0.187}\ (T_w/T_1)^{(-1.9792+0.3283\ \lg Re_1)}$$

for $Re_1 \geq 1.9 \cdot 10^4$

and by

$$St_T = 0.0085\ (T_w/T_1)^{-0.574} \qquad (13)$$

for $6 \cdot 10^3 \leq Re_1 \leq 1.9 \cdot 10^4$ /11/.

4.3 Roughness parameter of the velocity profile: R

The roughness parameters of the velocity profile, calculated from the transformed friction factor f_1 as

$$R(h^+) = \sqrt{\frac{2}{f_1}} - A_r \ln\left(\frac{\hat{y}}{h}\right) + \frac{A_r}{2}\,\frac{1+3\alpha/\beta}{1+\alpha/\beta} \qquad (14)$$

are plotted in figure 9 (A) versus the roughness Reynolds number

$$h^+ = \frac{h\,u_1^*}{\nu} \quad . \qquad (15)$$

With an increasing temperature ratio T_W/T_1 the R-values grow, at high h^+, however, only very little.

In figure 9 (B) the reduced R-values according to /3/

$$R(h_W^+)_{01} = R(h^+) - 0.4 \ln \left(\frac{h/\hat{y}}{0.01}\right) - \frac{5}{\sqrt{h_W^+}} \left(\frac{T_W}{T_1} - 1\right)^2 \qquad (16)$$

are plotted versus h_W^+.

For comparison three lines are shown. The correlation from /4/

$$R(h_W^+)_{01} = 4 + \frac{2.75}{h_W^+ + 0.256} \qquad (17)$$

and the correlation which was used in calculations with the SAGAPO code /1/

$$R(h_W^+)_{01} = 4.5 + \frac{5.5}{h_W^+ + 0.7} \qquad (18)$$

give somewhat higher R-values at high h_W^+-values. Although the friction factor results from /4/ were idendical with the present results the R-values are higher because the diameter of the rod was bigger. The correlation from /3/

$$R(h_W^+)_{01} = 1.04 \left(\frac{p-b}{h}\right)^{0.46} - \left[2 + \frac{7}{(p-b)/h}\right] \log \left(\frac{h}{b}\right) \qquad (19)$$

for $(p-b)/h \geq 6.3$

which was established for rectangular roughnesses gives R-values which agree very well with the present data for the isothermal runs.

In figure 9 (C) differently reduced R-values are shown. Meyer & Rehme /7/ proposed to calculate roughness parameters from the reduced friction factors as

$$R(h^+)_R = \sqrt{\frac{2}{f_{1R}}} - A_r \ln\left(\frac{\hat{y}}{h}\right) + \frac{A_r}{2}\,\frac{1+3\alpha/\beta}{1+\alpha/\beta} \tag{19}$$

and plot them versus

$$h^+_{WR} = \frac{h\, u^*_{1R}}{\nu_W} = h^+_W \sqrt{\left(\frac{T_W}{T_1}\right)^{0.29}} \quad . \tag{20}$$

These data are best correlated by

$$\begin{aligned} R(h^+)_R &= 4.85, && h^+_{WR} \geq 60 \\ R(h^+)_R &= 7.85 - 1.68 \log h^+_{WR}, && h^+_{WR} < 60 \end{aligned} \tag{21}$$

For a slope A_r=1.7 in the logarithmic velocity profile the R-values are higher by 1.95 at high h^+ (R=6.85) and by 1.7 at low h^+. Together with A_r = 1.7 this gives the friction factors f_1 which are between 1% and 3.3% smaller than with A_r=2.5. A R-value of R=6.85 with A_r=1.7 corresponds very well to the results from measurements in the rectangular channel at ribs with rounded edges /5/, where R=7.00 was found. The roughness was similar but bigger by a factor of 75. The present roughness has a somewhat smaller pitch. It is (p-b)/h=6.91 versus 7.14 in /5/. The lower value of R=6.85 compared to R=7.0 gives a higher friction factor. An increase of the friction factor with smaller p/h-ratios was also found in /5/ down to (p-b)/h=5.5.

4.4. Roughness parameter of the temperature profile: G

The roughness parameter of the logarithmic temperature profile

$$T^+ = A_r \ln \left(\frac{y}{h}\right) + G \qquad (22)$$

was calculated by different methods and reduced for the temperature, entrance, Prandtl number and relative roughness height effects. The equations which were applied are listed in the appendix.

Figure 10 shows G^+ and G^* versus h^+. The differences are small; for high h^+, G^+ is slightly higher than G^*, for very low h^+ the opposite is true. At approximately $h_W^+ = 10$, G^+ is equal G^*.

The reduced data GPRO1 are plotted in Fig.11, evaluated with $A_r = 2.5$ (A) and with $A_r = 1.7$ (B). The correlation from /3/ (with R_{O1}=4.35)

$$GPRO1 = 4.3\ h_W^{+\,0.246} \qquad (23)$$

fits very well for high h_w^+, but the minimum value of GPRO1 is 7.7 rather than 10. For the temperature reduction an exponent of 0.68 was used as it was found in /12/ for two-dimensional roughnesses.

The GPRO1 values evaluated with $A_r = 1.7$ are higher by approximately 2.7.

In figure 12 the reduced data G_R^* are plotted versus h_R^+. As for the Stanton number the temperature effect is overcompensated at high h^+. For low T_W/T_B-ratios it is

$$G_R^* = 5.77\ h_R^{+\,0.215} \geq 11.5 \qquad (24)$$

The data for $A_r = 1.7$ again are higher by 2.7.

The roughness parameter GTR1 which is transformed to the rough zone and reduced for the temperature and roughness height effects is plotted in figure 13. The temperature reduction is much better than for G_R^*. The data are best correlated by

$$GTR1 = 3.28\, h_R^{+0.262} + \frac{15}{h_R^+} \quad . \tag{25}$$

5. Conclusion

The comparison of the results of the present measurements with correlations derived from measurements at similar roughnesses and at rectangular roughnesses showed little difference in the friction factor, respectively the R-parameter and the Stanton number, respectively the G-parameter.

A calculation for BR2 typical parameters with helium,

$P/D = 1.41$
$h/D = 0.01425$
$Re = 5 \cdot 10^4$
$T_W/T_B = 1.1$

with the transformed GTR1-value according to equation (25) and $R(h^+)_R$ from Eq.(21) gave Stanton numbers 10% higher than with GPR01 from (23) and R_{01} from Eq.(18). For $T_W/T_B = 1.4$ the difference in the Stanton number was 5%. The differences for a calculation with air were higher by 1 percentage point.

Acknowledgements

The author would like to express his gratitude to Messrs. P. Durand and A. Roth for their cooperation in performing the experiments and making the drawings.

References

/1/ S. Cevolani and K. Rehme:
Forced convection heat transfer in a bundle of 12 rods, ANS-ASME Nuclear Reactor Thermal-Hydraulic 1980 Topical Meeting Saratoga, N.Y. (1980)

/2/ M. Dalle Donne, J. Marek, A. Martelli, K. Rehme:
BR2 Bundle mockup heat transfer experiments, Nuclear Engng. Design 40, pp.143-156 (1977)

/3/ M. Dalle Donne and L. Meyer:
Turbulent convective heat transfer from rough surfaces with two-dimensional rectangular ribs, Int. J. Heat Mass Transfer 20, pp.583-620 (1977)

/4/ M. Dalle Donne, M. Hudina, M. Huggenberger, L. Meyer, K. Rehme:
EIR, KfK joint heat transfer experiment on a single rod, roughened with trapezoidal rounded ribs and cooled by various gases. KfK-Report 2674, EUR 5755e, EIR-Report 349 (1978)

/5/ L. Meyer and L. Vogel:
The velocity distribution and pressure loss at artificial roughnesses with sharp and rounded edges, KfK-Report 2885 (1979)

/6/ K. Rehme:
The structure of turbulent flow through a wall subchannel of a rod bundle with roughened rods, KfK-Report 2716 (1978)

/7/ L. Meyer and K. Rehme:
Heat transfer and pressure drop measurements with roughened single pins cooled by various gases, KfK-Report 2980 (1980)

/8/ M. Dalle Donne and L. Meyer:
Heat transfer and friction coefficients for air flow in a smooth annulus, KfK-Report 2837 (1979)

/9/ M. Hudina and S. Janar:
The influence of heat conduction on the heat transfer performance of some ribbed surfaces tested in ROHAN experiment, EIR-Report TM-IN-572 (1974)

/10/ R.J. Firth:
A method for analyzing heat transfer and pressure drop data obtained from partially roughened annular channels, 5th NEA-GCFR Heat Transfer Specialists Meeting, Würenlingen, (1979)

/11/ M. Dalle Donne, personal communication.

/12/ M. Dalle Donne, L. Meyer:
Convective heat transfer from rough surfaces with two-dimensional ribs: transitional and laminar flow, KfK-Report 2566 (1978)

Appendix

Equations for the roughness parameter G

$$G^* = \frac{1}{St_B}\sqrt{\frac{f_1}{2}}\,\frac{u_1}{u_B} - A_r \ln\left(\frac{1-\alpha}{h/r_2}\right) + \frac{A_r}{2}\,\frac{(1+3\alpha)}{(1+\alpha)} \qquad \text{(A-1)}$$

$$G_R^* = \frac{1}{St_{BR}}\sqrt{\frac{f_1}{2}}\sqrt{\left(\frac{T_W}{T_1}\right)^{0.29}}\,\frac{u_1}{u_B} - A_r \ln\left(\frac{1-\alpha}{h/r_2}\right) + \frac{A_r}{2}\,\frac{(1+3\alpha)}{(1+\alpha)} \qquad \text{(A-2)}$$

with

$$St_{BR} = \frac{St_B}{1 + 14Re_B^{-0.35}\,\lg\left[4.35\left(\frac{x}{D_h}\right)^{-.6}\right]}\left(\frac{T_W}{T_B}\right)^{-ex} Pr^{0.6} \qquad \text{(A-3)}$$

The denominator in (A-3) is set to 1, if it becomes smaller than 1.

$$G^+ = \frac{(T_W - T_{W2})\,\rho_B\,c_{pB}\,u_1^*}{q_1} - A_r \ln\left(\frac{1-\alpha}{h/r_2}\right) \qquad \text{(A-4)}$$

$$GPRO1 = \frac{G^+}{Pr^{0.44}\left(\frac{T_W}{T_B}\right)^{0.68}\left(\frac{h}{0.01(r_2-r_1)}\right)^{0.053}} \qquad \text{(A-5)}$$

$$G_T = \frac{\sqrt{f_1/2}}{St_{1T}} - A_r \ln\left(\frac{\beta-\alpha}{h/r_2}\right) + \frac{A_r}{2}\,\frac{(1+3\alpha/\beta)}{(1+\alpha/\beta)} \qquad \text{(A-6)}$$

St_{1T} is the Stanton number transformed with the method proposed in /7/.

$$G_{TR} = \frac{\sqrt{\frac{f_{1R}}{2}}}{St_{1TR}} - A_r \ln\left(\frac{\beta-\alpha}{h/r_2}\right) + \frac{A_r}{2}\frac{(1+3\alpha/\beta)}{(1+\alpha/\beta)} \qquad \text{(A-7)}$$

with

$$St_{1TR} = \frac{St_{1T}}{1 + 14Re_1^{-0.35}\left[\lg 4.35\left(\frac{x}{D_1}\right)^{-.6}\right]}\left(\frac{T_W}{T_1}\right)^{-ex} Pr^{0.6} \qquad \text{(A-8)}$$

and $$f_{1R} = f_1\left(\frac{T_W}{T_1}\right)^{0.29} \qquad \text{(A-9)}$$

$$GTR1 = GTR\left(\frac{h}{0.01\ \hat{y}}\right)^{-0.2} \qquad \text{(A-10)}$$

$$G_{TF} = \frac{\sqrt{f_1/2}}{St_{1F}} - A_r \ln\left(\frac{\beta-\alpha}{h/r_2}\right) + \frac{A_r}{2}\frac{(1+3\alpha/\beta)}{(1+\alpha/\beta)} \qquad \text{(A-11)}$$

with /10/,

$$St_{1F} = St\left[\frac{f_1 D_h}{D_1 F}\right]^{0.5}\left[1 + \frac{9}{(1+D_1/8r_1)}St_1\frac{(1-\beta^2)}{(1-\alpha^2)}\sqrt{\frac{2}{f_1}}\right] \qquad \text{(A-12)}$$

G_{TFR} is calculated with St_{1F}, (A-8), (A-9) and (A-11).

Nomenclature

A	area of flow cross-section (m^2)
A_r	slope of the logarithmic velocity and temperature profile
b	width of the ribs (m)
Bi	Biot number ($=\alpha h/k_c$)
c_p	specific heat at constant pressure ($Ws\ kg^{-1}\ K^{-1}$)
D_h, D_1	hydraulic diameter (m)
D_o	outer diameter of annulus (m)
f	friction factor ($=2\tau/\rho u^2$)
G	parameter in the logarithmic temperature profile for rough surfaces
h	height of the roughness ribs (m)
h^+	dimensionless height of the rib or roughness Reynolds number ($=h\ u^*/\nu$)
k_c	thermal conductivity of the test rod ($Wm^{-1}\ K^{-1}$)
l	heated length of the test rods (m)
$\dot{m}$	mass flow ($kg\ s^{-1}$)
Nu	Nusselt number
p	pitch of the roughness ribs (m)
Pr	Prandtl number
q	heat flux (Wm^{-2})
r	radius (m)
$R(h^+)$	parameter in the logarithmic velocity profile for rough surfaces
Re	Reynolds number ($=u\ D_h/\nu$)
St	Stanton number ($=\alpha/(\rho u c_p)=Nu/RePr$)
T	temperature (K)
T^+	dimensionless temperature ($=(T_W-T)\rho c_p u^*/q$)
u	gas velocity (ms^{-1})
u^*	friction velocity ($=\sqrt{\tau/\rho}$) (ms^{-1})
u^+	dimensionless velocity ($=u/u^*$)
x	axial length starting at the beginning of the heating of the rod (m)
$\hat{y}$	radial distance of zero shear stress plane from the rough wall

α	convective heat transfer coefficient ($Wm^{-2}\ K^{-1}$)
α	r_1/r_2
β	r_o/r_2
ε	emissivity coefficient
ν	kinematic viscosity ($m^2\ s^{-1}$)
ρ	density of the gas ($kg\ m^{-3}$)
τ	shear stress at the wall (Nm^{-2})

Subscripts

B	bulk or total of the annular cross-section
1	inner rough zone of channel
2	outer smooth zone of channel
W	wall
o	zero shear position
vol	volumetric radius of rough rod
c	corrected
M	measured
R	reduced (for temperature effect)
r	rough
s	smooth

Nomenclature of the tables (where not self-explaining)

STPR Eq.(A-3)

$$ST1+/ = \left(\frac{St_1}{St_B}\right)^+ = \frac{\frac{1}{St_B}\sqrt{\frac{f_1}{2}}}{G^+ + 2.5\ \ln\left(\frac{\beta-\alpha}{h/r_2}\right) - \frac{A_r}{2}\frac{(1+3\alpha/\beta)}{(1+\alpha/\beta)}}$$

$$ST1*/ = \left(\frac{St_1}{St_B}\right)^* = \frac{\frac{1}{St_B}\sqrt{\frac{f_1}{2}}}{G^* + 2.5\ \ln\left(\frac{\beta-\alpha}{h/r_2}\right) - \frac{A_r}{2}\frac{1+3\alpha/\beta}{1+\alpha/\beta}}$$

$STT+/ = St_{1T}/St_B$, transformed with G^+ /7/

$STT*/ = St_{1T}/St_B$, transformed with G^* /7/

$ST1F/ = St_{1F}/St_B$ St_{1F} from Eq. (A-12)

$$X = \ln\left(\frac{\hat{y}}{h}\right) - \frac{1}{2}\frac{3+\beta/\alpha}{1+\beta/\alpha}$$

$$Y_R = \sqrt{2/f_1}$$

$$Y_G = \sqrt{2/f_1}/St_{1F}$$

Symbols in the plots

□ isothermal runs

○ ↓ thermal runs, increasing T_W/T_B-ratio

△ ↓ with arrow; the exact T_W/T_B-ratios

◇ ↓ can be taken from the tables.

VERS. NR.	RE*E4	RE1*E4	F	F1	STB	STPR	F1/F2	TW/TB	TW/T1	PR	H/Y	BETA	H+	H+W	H+R	H+RW	RH+	RH+W1	RH+R
5-16- 1	20.22	34.56	.00840	.01641	.00388	.00347	3.60	1.36	1.34	.706	.0410	.834	238.2	144.2	248.4	150.4	5.23	4.67	4.78
5-16- 2	16.24	27.31	.00841	.01626	.00414	.00369	3.43	1.35	1.34	.706	.0416	.829	190.8	115.4	199.0	120.4	5.33	4.76	4.87
5-16- 3	13.10	21.29	.00834	.01558	.00413	.00369	3.17	1.36	1.34	.706	.0426	.821	150.0	90.4	156.5	94.3	5.63	5.05	5.16
5-16- 4	10.64	16.92	.00852	.01556	.00435	.00387	3.04	1.35	1.32	.706	.0432	.816	121.1	75.0	126.0	78.1	5.68	5.10	5.24
5-16- 5	8.84	13.90	.00874	.01581	.00444	.00396	2.98	1.35	1.32	.706	.0435	.814	101.2	62.6	105.4	65.2	5.60	5.02	5.16
5-16- 6	7.12	10.99	.00892	.01589	.00458	.00409	2.87	1.36	1.32	.705	.0441	.810	81.5	50.3	84.9	52.4	5.61	5.02	5.17
5-16- 7	5.96	8.85	.00878	.01508	.00472	.00421	2.64	1.36	1.32	.705	.0453	.801	66.2	41.0	68.9	42.7	5.99	5.39	5.54
5-16- 8	4.95	7.27	.00901	.01533	.00482	.00430	2.58	1.36	1.32	.705	.0457	.799	55.4	34.5	57.6	35.9	5.91	5.31	5.47
5-16- 9	3.64	5.17	.00925	.01523	.00502	.00447	2.40	1.36	1.31	.704	.0468	.791	40.5	25.4	42.1	26.4	6.02	5.40	5.58
5-16- 10	2.50	3.26	.00917	.01390	.00508	.00455	2.04	1.37	1.31	.703	.0498	.773	26.3	16.4	27.4	17.1	6.72	6.08	6.25
5-16- 11	2.45	3.28	.00945	.01466	.00514	.00458	2.13	1.36	1.31	.703	.0490	.778	26.6	16.7	27.7	17.4	6.36	5.72	5.91
5-16- 12	2.20	2.91	.00952	.01455	.00515	.00459	2.07	1.36	1.30	.703	.0495	.775	23.9	15.1	24.8	15.7	6.44	5.80	5.99
5-16- 13	1.79	2.34	.00976	.01474	.00532	.00472	2.00	1.34	1.29	.703	.0502	.771	19.6	12.6	20.4	13.0	6.40	5.75	5.97
5-16- 14	1.49	1.86	.00986	.01421	.00532	.00472	1.85	1.34	1.29	.703	.0517	.763	15.9	10.3	16.5	10.7	6.69	6.04	6.27
5-16- 15	1.20	1.48	.01024	.01444	.00539	.00477	1.78	1.33	1.28	.703	.0525	.759	12.9	8.5	13.4	8.8	6.63	5.97	6.23
5-16- 16	1.00	1.18	.01031	.01392	.00530	.00472	1.65	1.35	1.29	.703	.0542	.750	10.6	6.9	11.0	7.1	6.95	6.27	6.52
5-16- 17	0.80	0.90	.01060	.01375	.00533	.00473	1.54	1.34	1.27	.703	.0558	.743	8.3	5.5	8.6	5.7	7.10	6.41	6.68
5-16- 18	0.67	0.73	.01071	.01323	.00527	.00467	1.42	1.34	1.27	.703	.0577	.735	6.9	4.5	7.1	4.7	7.43	6.73	7.01
5-16- 19	0.55	0.58	.01102	.01316	.00514	.00457	1.34	1.35	1.27	.703	.0593	.729	5.6	3.7	5.9	3.9	7.56	6.84	7.13
5-16- 20	10.44	15.49	.00846	.01585	.00406	.00416	3.14	1.84	1.76	.699	.0439	.813	114.3	43.9	124.0	47.7	5.62	5.02	4.73
5-16- 21	3.11	3.73	.00872	.01349	.00451	.00453	2.11	1.78	1.64	.698	.0506	.770	30.3	13.1	32.5	14.1	6.95	6.30	6.10
5-16- 22	2.52	2.94	.00888	.01326	.00457	.00456	1.99	1.76	1.61	.698	.0518	.763	24.3	10.8	26.1	11.6	7.12	6.46	6.29
5-16- 23	2.00	2.21	.00897	.01273	.00462	.00460	1.82	1.76	1.60	.698	.0538	.754	18.8	8.5	20.1	9.1	7.47	6.79	6.65
5-16- 24	1.88	2.02	.00892	.01235	.00466	.00463	1.74	1.74	1.58	.699	.0548	.749	17.3	8.0	18.5	8.6	7.71	7.03	6.90
5-16- 25	1.55	1.61	.00914	.01223	.00464	.00462	1.65	1.75	1.58	.699	.0561	.743	14.1	6.5	15.0	7.0	7.84	7.15	7.02
5-16- 26	1.21	1.23	.00951	.01235	.00473	.00469	1.57	1.74	1.56	.698	.0573	.738	11.1	5.2	11.8	5.6	7.83	7.14	7.04
5-16- 27	1.00	0.98	.00981	.01234	.00467	.00463	1.49	1.74	1.55	.698	.0585	.733	9.1	4.3	9.7	4.6	7.89	7.19	7.11
5-16- 28	0.89	0.90	.01038	.01353	.00487	.00482	1.58	1.74	1.56	.697	.0571	.739	8.5	4.0	9.1	4.3	7.25	6.56	6.49
5-16- 29	5.96	7.65	.00808	.01322	.00425	.00431	2.38	1.80	1.67	.702	.0483	.783	58.1	24.4	62.6	26.3	6.94	6.31	6.06
5-16- 30	4.19	5.07	.00823	.01287	.00442	.00447	2.16	1.80	1.65	.701	.0503	.772	39.9	17.1	42.9	18.3	7.22	6.57	6.34
5-16- 31	3.06	3.57	.00853	.01283	.00457	.00458	2.01	1.76	1.62	.700	.0516	.764	29.0	12.9	31.0	13.8	7.31	6.66	6.47
5-16- 32	21.08	37.25	.00866	.01720	.00402	.00358	3.76	1.34	1.33	.706	.0403	.839	257.3	156.3	268.3	163.0	4.93	4.37	4.49
5-16- 33	19.32	31.59	.00842	.01711	.00379	.00389	3.78	1.85	1.81	.701	.0414	.832	225.0	82.7	245.2	90.1	5.03	4.46	4.14
5-16- 34	14.06	21.86	.00844	.01640	.00396	.00405	3.42	1.84	1.77	.700	.0426	.822	158.2	60.4	171.8	65.6	5.34	4.76	4.47
5-16- 35	11.19	16.70	.00839	.01578	.00408	.00417	3.17	1.84	1.75	.700	.0437	.814	122.4	47.3	132.8	51.3	5.63	5.04	4.75
5-16- 36	8.30	11.79	.00838	.01510	.00419	.00427	2.87	1.82	1.72	.700	.0452	.803	88.1	35.0	95.3	37.9	5.97	5.37	5.10
5-16- 37	6.21	8.52	.00855	.01493	.00432	.00437	2.68	1.80	1.70	.699	.0463	.796	65.2	26.6	70.4	28.7	6.10	5.48	5.24
5-16- 38	4.59	5.93	.00856	.01415	.00441	.00444	2.40	1.78	1.67	.699	.0482	.784	46.4	19.6	50.0	21.1	6.52	5.90	5.68
5-16- 39	3.84	4.75	.00852	.01350	.00442	.00443	2.21	1.77	1.65	.698	.0496	.775	37.7	16.2	40.5	17.5	6.89	6.25	6.04
5-16- 40	17.60	26.08	.00811	.01581	.00356	.00409	3.48	2.25	2.11	.697	.0430	.820	187.8	54.0	209.2	60.2	5.58	4.99	4.42
5-16- 41	13.61	19.38	.00813	.01547	.00372	.00426	3.26	2.24	2.09	.696	.0441	.813	142.1	41.7	158.1	46.3	5.77	5.17	4.61
5-16- 42	10.16	13.62	.00805	.01461	.00379	.00433	2.93	2.23	2.05	.696	.0457	.801	101.6	30.7	112.8	34.1	6.20	5.59	5.04
5-16- 43	7.51	9.41	.00799	.01370	.00385	.00437	2.60	2.21	2.00	.696	.0477	.788	71.7	22.5	79.3	24.9	6.69	6.07	5.53
5-16- 44	5.69	6.78	.00806	.01316	.00396	.00443	2.37	2.16	1.94	.696	.0494	.778	52.8	17.5	58.1	19.2	7.03	6.39	5.90
5-16- 45	4.28	4.64	.00795	.01191	.00392	.00439	2.04	2.17	1.91	.695	.0525	.761	37.0	12.6	40.6	13.9	7.83	7.17	6.67
5-16- 46	3.48	3.57	.00802	.01138	.00400	.00444	1.86	2.13	1.85	.695	.0545	.752	29.1	10.4	31.8	11.4	8.23	7.55	7.09
5-16- 47	13.35	23.69	.00914	.01760	.0	.0	3.50	1.00	1.00	.709	.0407	.835	167.6	167.6	167.6	167.6	4.83	4.27	4.83
5-16- 48	10.24	17.80	.00925	.01740	.0	.0	3.29	1.00	1.00	.709	.0414	.829	128.0	128.0	128.0	128.0	4.94	4.37	4.94
5-16- 49	8.42	14.45	.00941	.01747	.0	.0	3.18	1.00	1.00	.708	.0419	.826	105.5	105.5	105.5	105.5	4.95	4.38	4.95
5-16- 50	6.78	11.46	.00958	.01747	.0	.0	3.04	1.00	1.00	.708	.0424	.821	85.0	85.0	85.0	85.0	4.99	4.41	4.99

VERS.NR.	RE*E4	Q<KW/M2>	ST1+/	ST1*/	STT+/	STT*/	ST1F/	1+	G+	GPRD1	G*	G*R	GT	GTR	GTR1	GTF	GTFR	X	YR	YG
5-16- 1	20.22	205.5	1.08	1.08	1.10	1.11	1.17	238.2	15.8	14.2	15.7	19.5	15.3	19.2	14.5	14.2	17.9	2.32	11.04	20.0
5-16- 2	16.24	175.5	1.07	1.10	1.10	1.12	1.19	190.8	14.6	13.1	14.1	17.7	14.1	17.8	13.3	12.5	16.1	2.31	11.09	18.3
5-16- 3	13.10	145.8	1.08	1.09	1.11	1.12	1.20	153.6	14.1	12.6	13.8	17.3	13.6	17.2	12.8	12.2	15.6	2.28	11.33	17.9
5-16- 4	10.64	120.1	1.10	1.09	1.13	1.12	1.21	121.1	12.8	11.5	12.9	16.2	12.3	15.7	11.7	11.1	14.4	2.27	11.34	16.8
5-16- 5	8.84	103.0	1.10	1.09	1.13	1.12	1.21	101.2	12.5	11.3	12.6	15.9	12.0	15.4	11.4	10.9	14.1	2.26	11.25	16.5
5-16- 6	7.12	87.4	1.11	1.10	1.14	1.13	1.23	81.5	12.0	10.7	12.1	15.2	11.5	14.7	10.9	10.3	13.4	2.24	11.22	15.9
5-16- 7	5.96	76.5	1.12	1.10	1.15	1.14	1.25	66.2	11.0	9.8	11.1	14.1	10.5	13.5	9.9	9.2	12.1	2.21	11.52	14.7
5-16- 8	4.95	64.3	1.12	1.11	1.15	1.14	1.26	55.4	10.7	9.6	10.9	13.8	10.2	13.2	9.7	8.9	11.8	2.20	11.42	14.4
5-16- 9	3.64	49.6	1.13	1.11	1.17	1.15	1.28	40.5	10.0	9.0	10.2	13.0	9.5	12.3	9.0	8.2	11.0	2.18	11.46	13.6
5-16- 10	2.50	35.7	1.15	1.12	1.19	1.16	1.32	26.3	9.0	8.1	9.4	12.0	8.5	11.1	8.1	7.1	9.7	2.11	11.99	12.4
5-16- 11	2.45	34.5	1.14	1.12	1.18	1.16	1.31	26.6	9.3	8.3	9.6	12.3	8.8	11.5	8.3	7.4	10.0	2.13	11.68	12.7
5-16- 12	2.20	30.7	1.14	1.12	1.18	1.16	1.32	23.9	9.2	8.3	9.5	12.2	8.7	11.4	8.3	7.3	9.9	2.12	11.72	12.6
5-16- 13	1.79	24.8	1.14	1.13	1.18	1.17	1.34	19.6	9.0	8.1	9.0	11.7	8.5	11.1	8.0	6.8	9.5	2.10	11.65	12.1
5-16- 14	1.49	20.9	1.16	1.13	1.20	1.17	1.35	15.9	8.5	7.7	8.9	11.5	8.0	10.5	7.6	6.5	9.1	2.07	11.86	11.7
5-16- 15	1.20	16.2	1.17	1.13	1.21	1.17	1.36	12.9	8.4	7.7	8.8	11.5	7.9	10.4	7.5	6.5	9.1	2.05	11.77	11.6
5-16- 16	1.00	14.2	1.18	1.13	1.22	1.18	1.37	10.6	8.4	7.6	8.9	11.5	7.9	10.4	7.4	6.4	8.9	2.02	11.99	11.5
5-16- 17	0.80	11.0	1.19	1.14	1.23	1.18	1.39	8.3	8.2	7.5	8.7	11.4	7.7	10.2	7.2	6.2	8.8	1.99	12.06	11.2
5-16- 18	0.67	9.1	1.20	1.14	1.24	1.18	1.41	6.9	8.1	7.4	8.7	11.3	7.6	10.0	7.1	6.1	8.6	1.95	12.29	11.0
5-16- 19	0.55	7.5	1.20	1.14	1.24	1.18	1.41	5.6	8.5	7.7	9.1	11.8	8.0	10.4	7.3	6.4	9.0	1.92	12.33	11.2
5-16- 20	10.44	302.6	1.10	1.10	1.13	1.13	1.23	114.3	14.4	10.5	14.3	15.6	13.9	15.9	11.9	12.2	13.5	2.25	11.23	17.9
5-16- 21	3.11	95.0	1.14	1.11	1.17	1.15	1.32	30.3	10.9	8.1	11.2	12.4	10.3	12.3	8.9	8.5	9.7	2.09	12.18	13.7
5-16- 22	2.52	75.8	1.14	1.11	1.18	1.15	1.34	24.3	10.5	7.9	10.9	12.2	10.0	11.9	8.6	8.1	9.4	2.07	12.28	13.3
5-16- 23	2.00	60.6	1.15	1.12	1.20	1.16	1.36	18.8	10.0	7.6	10.5	11.7	9.5	11.4	8.1	7.6	8.8	2.03	12.53	12.7
5-16- 24	1.88	55.8	1.16	1.12	1.21	1.16	1.38	17.3	9.6	7.3	10.1	11.4	9.1	10.9	7.8	7.2	8.4	2.01	12.72	12.2
5-16- 25	1.55	46.4	1.17	1.12	1.21	1.16	1.39	14.1	9.6	7.3	10.2	11.4	9.1	11.0	7.8	7.2	8.3	1.98	12.79	12.1
5-16- 26	1.21	36.6	1.17	1.12	1.22	1.16	1.40	11.1	9.4	7.2	10.1	11.3	8.9	10.7	7.6	6.9	8.1	1.96	12.73	11.8
5-16- 27	1.00	30.0	1.17	1.11	1.22	1.15	1.40	9.1	9.7	7.4	10.4	11.6	9.1	11.0	7.7	7.2	8.4	1.94	12.73	12.0
5-16- 28	0.89	28.4	1.17	1.11	1.21	1.15	1.39	8.5	9.7	7.4	10.4	11.7	9.2	11.1	7.8	7.2	8.5	1.96	12.16	12.2
5-16- 29	5.96	172.3	1.12	1.10	1.16	1.14	1.29	58.1	11.7	8.7	12.0	13.2	11.2	13.1	9.6	9.5	10.6	2.14	12.30	14.9
5-16- 30	4.19	126.1	1.13	1.11	1.17	1.15	1.32	39.9	10.8	8.0	11.1	12.2	10.2	12.1	8.7	8.4	9.5	2.10	12.47	13.7
5-16- 31	3.06	91.4	1.14	1.11	1.19	1.15	1.35	29.0	10.2	7.7	10.6	11.8	9.6	11.5	8.3	7.8	9.0	2.07	12.49	13.0
5-16- 32	21.08	216.2	1.06	1.08	1.08	1.11	1.16	257.3	15.9	14.4	15.5	19.3	15.5	19.4	14.7	14.0	17.8	2.34	10.78	19.9
5-16- 33	19.32	522.2	1.08	1.10	1.11	1.13	1.20	225.0	16.8	12.3	16.4	17.8	16.3	18.5	13.9	14.7	16.0	2.31	10.81	20.4
5-16- 34	14.06	394.1	1.09	1.10	1.12	1.13	1.21	158.2	15.3	11.2	15.1	16.5	14.8	16.9	12.7	13.2	14.5	2.28	11.04	18.9
5-16- 35	11.19	325.7	1.10	1.10	1.13	1.13	1.23	122.4	14.2	10.4	14.1	15.4	13.7	15.8	11.7	12.1	13.3	2.25	11.26	17.7
5-16- 36	8.30	242.2	1.10	1.10	1.14	1.14	1.25	88.1	13.2	9.8	13.2	14.5	12.7	14.9	10.9	11.0	12.3	2.22	11.51	16.6
5-16- 37	6.21	183.4	1.11	1.11	1.14	1.14	1.27	65.2	12.5	9.3	12.6	13.9	12.0	14.1	10.4	10.3	11.6	2.19	11.57	15.8
5-16- 38	4.59	135.8	1.12	1.11	1.16	1.15	1.29	46.4	11.7	8.7	11.8	13.1	11.1	13.1	9.6	9.4	10.7	2.15	11.89	14.8
5-16- 39	3.84	112.2	1.13	1.11	1.17	1.15	1.31	37.7	11.2	8.4	11.5	12.8	10.7	12.7	9.2	8.9	10.2	2.11	12.17	14.2
5-16- 40	17.60	727.0	1.09	1.09	1.12	1.11	1.21	187.8	17.2	11.0	17.3	16.6	16.7	17.6	13.2	15.0	14.3	2.27	11.25	20.7
5-16- 41	13.61	589.6	1.10	1.09	1.12	1.12	1.23	142.1	16.0	10.3	16.1	15.4	15.5	16.4	12.2	13.7	13.0	2.24	11.37	19.3
5-16- 42	10.16	443.0	1.10	1.09	1.13	1.12	1.25	101.6	14.9	9.6	15.1	14.5	14.4	15.4	11.4	12.5	11.9	2.20	11.70	18.0
5-16- 43	7.51	327.6	1.11	1.09	1.14	1.13	1.27	71.7	14.0	9.1	14.3	13.7	13.5	14.5	10.6	11.5	11.0	2.16	12.08	16.9
5-16- 44	5.69	243.4	1.12	1.10	1.15	1.13	1.30	52.8	13.1	8.6	13.4	13.1	12.5	13.7	9.9	10.5	10.2	2.12	12.33	15.8
5-16- 45	4.28	184.7	1.13	1.09	1.16	1.13	1.32	37.0	12.4	8.2	13.0	12.6	11.9	13.0	9.3	9.7	9.4	2.05	12.96	14.9
5-16- 46	3.48	148.8	1.14	1.09	1.18	1.13	1.35	29.1	11.7	7.7	12.4	12.1	11.1	12.3	8.8	9.0	8.7	2.01	13.26	14.0
5-16- 47	13.35	0.0	0.0	0.0	0.0	0.0	0.0	167.6	0.0	0.0	0.0	0.0	0.0	0.0	0.0	0.0	0.0	2.33	10.66	0.0
5-16- 48	10.24	0.0	0.0	0.0	0.0	0.0	0.0	128.0	0.0	0.0	0.0	0.0	0.0	0.0	0.0	0.0	0.0	2.31	10.72	0.0
5-16- 49	8.42	0.0	0.0	0.0	0.0	0.0	0.0	105.5	0.0	0.0	0.0	0.0	0.0	0.0	0.0	0.0	0.0	2.30	10.70	0.0
5-16- 50	6.78	0.0	0.0	0.0	0.0	0.0	0.0	85.0	0.0	0.0	0.0	0.0	0.0	0.0	0.0	0.0	0.0	2.29	10.70	0.0

VERS.NR.	RE*E4	RE1*E4	F	F1	STB	STPR	F1/F2	TW/T8	TW/T1	PR	H/Y	BETA	H+	H+W	H+R	H+RW	RH+	RH+01	RH+R
5-16- 51	5.69	9.50	.00973	.01751	.0	.0	2.94	1.00	1.00	.708	.0428	.818	71.4	71.4	71.4	71.4	5.00	4.42	5.00
5-16- 52	4.81	7.94	.00991	.01760	.0	.0	2.86	1.00	1.00	.708	.0432	.815	60.6	60.6	60.6	60.6	5.00	4.41	5.00
5-16- 53	3.99	6.48	.01005	.01752	.0	.0	2.74	1.00	1.00	.707	.0438	.810	50.2	50.2	50.2	50.2	5.06	4.47	5.06
5-16- 54	4.31	6.98	.00981	.01705	.0	.0	2.71	1.00	1.00	.708	.0439	.810	53.4	53.4	53.4	53.4	5.21	4.62	5.21
5-16- 55	3.27	5.18	.01006	.01703	.0	.0	2.56	1.00	1.00	.709	.0448	.804	40.6	40.6	40.6	40.6	5.27	4.67	5.27
5-16- 56	3.13	4.95	.01013	.01710	.0	.0	2.54	1.00	1.00	.709	.0449	.803	38.9	38.9	38.9	38.9	5.25	4.65	5.25
5-16- 57	2.71	4.23	.01032	.01721	.0	.0	2.47	1.00	1.00	.709	.0453	.800	33.8	33.8	33.8	33.8	5.24	4.64	5.24
5-16- 58	2.65	4.17	.01048	.01762	.0	.0	2.52	1.00	1.00	.708	.0450	.802	33.5	33.5	33.5	33.5	5.10	4.50	5.10
5-16- 59	2.42	3.75	.01043	.01719	.0	.0	2.41	1.00	1.00	.708	.0457	.798	30.2	30.2	30.2	30.2	5.27	4.67	5.27
5-16- 60	2.23	3.42	.01047	.01705	.0	.0	2.35	1.00	1.00	.708	.0461	.795	27.8	27.8	27.8	27.8	5.34	4.73	5.34
5-16- 61	1.83	2.74	.01056	.01667	.0	.0	2.20	1.00	1.00	.708	.0471	.788	22.6	22.6	22.6	22.6	5.52	4.90	5.52
5-16- 62	1.32	1.90	.01076	.01612	.0	.0	1.98	1.00	1.00	.709	.0489	.777	16.1	16.1	16.1	16.1	5.81	5.18	5.81
5-16- 63	1.12	1.56	.01091	.01587	.0	.0	1.87	1.00	1.00	.709	.0499	.772	13.5	13.5	13.5	13.5	5.95	5.31	5.95
5-16- 64	0.93	1.27	.01113	.01574	.0	.0	1.78	1.00	1.00	.708	.0509	.766	11.2	11.2	11.2	11.2	6.06	5.41	6.06
5-16- 65	0.76	1.02	.01129	.01537	.0	.0	1.66	1.00	1.00	.708	.0523	.759	9.1	9.1	9.1	9.1	6.27	5.60	6.27
5-16- 66	0.66	0.85	.01127	.01470	.0	.0	1.53	1.00	1.00	.708	.0539	.751	7.8	7.8	7.8	7.8	6.61	5.94	6.61
5-16- 67	0.55	0.68	.01133	.01401	.0	.0	1.40	1.00	1.00	.707	.0560	.741	6.3	6.3	6.3	6.3	7.01	6.32	7.01
5-16- 68	0.48	0.57	.01128	.01322	.0	.0	1.28	1.00	1.00	.707	.0584	.731	5.4	5.4	5.4	5.4	7.53	6.82	7.53
5-16- 69	0.39	0.42	.01100	.01142	.0	.0	1.05	1.00	1.00	.708	.0645	.710	4.1	4.1	4.1	4.1	8.88	8.14	8.88
5-16- 70	0.34	0.31	.01006	.00832	.0	.0	0.76	1.00	1.00	.708	.0749	.678	3.1	3.1	3.1	3.1	11.37	10.56	11.37
5-16- 71	16.49	29.45	.00884	.01711	.0	.0	3.55	1.00	1.00	.710	.0405	.836	204.3	204.3	204.3	204.3	4.97	4.41	4.97
5-16- 72	20.31	36.69	.00869	.01703	.0	.0	3.67	1.00	1.00	.710	.0402	.840	250.9	250.9	250.9	250.9	4.97	4.42	4.97
5-16- 73	21.81	39.94	.00885	.01763	.0	.0	3.84	1.00	1.00	.710	.0397	.844	273.9	273.9	273.9	273.9	4.76	4.21	4.76

AR =2.50

VERS.NR.	RE*E4	Q<KW/M2>	ST1+/	ST1*/	STT+/	STT*/	ST1F/	H+	G+	GPR01	G*	G*R	GT	GTR	GTR1	GTF	GTFR	X	YR	YG
5-16- 51	5.69	0.0	0.0	0.0	0.0	0.0	0.0	71.4	0.0	0.0	0.0	0.0	0.0	0.0	0.0	0.0	0.0	2.27	10.69	0.0
5-16- 52	4.81	0.0	0.0	0.0	0.0	0.0	0.0	60.6	0.0	0.0	0.0	0.0	0.0	0.0	0.0	0.0	0.0	2.26	10.66	0.0
5-16- 53	3.99	0.0	0.0	0.0	0.0	0.0	0.0	50.2	0.0	0.0	0.0	0.0	0.0	0.0	0.0	0.0	0.0	2.25	10.68	0.0
5-16- 54	4.31	0.0	0.0	0.0	0.0	0.0	0.0	53.4	0.0	0.0	0.0	0.0	0.0	0.0	0.0	0.0	0.0	2.25	10.83	0.0
5-16- 55	3.27	0.0	0.0	0.0	0.0	0.0	0.0	40.6	0.0	0.0	0.0	0.0	0.0	0.0	0.0	0.0	0.0	2.23	10.84	0.0
5-16- 56	3.13	0.0	0.0	0.0	0.0	0.0	0.0	38.9	0.0	0.0	0.0	0.0	0.0	0.0	0.0	0.0	0.0	2.22	10.81	0.0
5-16- 57	2.71	0.0	0.0	0.0	0.0	0.0	0.0	33.8	0.0	0.0	0.0	0.0	0.0	0.0	0.0	0.0	0.0	2.21	10.78	0.0
5-16- 58	2.65	0.0	0.0	0.0	0.0	0.0	0.0	33.5	0.0	0.0	0.0	0.0	0.0	0.0	0.0	0.0	0.0	2.22	10.65	0.0
5-16- 59	2.42	0.0	0.0	0.0	0.0	0.0	0.0	30.2	0.0	0.0	0.0	0.0	0.0	0.0	0.0	0.0	0.0	2.21	10.79	0.0
5-16- 60	2.23	0.0	0.0	0.0	0.0	0.0	0.0	27.8	0.0	0.0	0.0	0.0	0.0	0.0	0.0	0.0	0.0	2.20	10.83	0.0
5-16- 61	1.83	0.0	0.0	0.0	0.0	0.0	0.0	22.6	0.0	0.0	0.0	0.0	0.0	0.0	0.0	0.0	0.0	2.17	10.95	0.0
5-16- 62	1.32	0.0	0.0	0.0	0.0	0.0	0.0	16.1	0.0	0.0	0.0	0.0	0.0	0.0	0.0	0.0	0.0	2.13	11.14	0.0
5-16- 63	1.12	0.0	0.0	0.0	0.0	0.0	0.0	13.5	0.0	0.0	0.0	0.0	0.0	0.0	0.0	0.0	0.0	2.11	11.22	0.0
5-16- 64	0.93	0.0	0.0	0.0	0.0	0.0	0.0	11.2	0.0	0.0	0.0	0.0	0.0	0.0	0.0	0.0	0.0	2.09	11.27	0.0
5-16- 65	0.76	0.0	0.0	0.0	0.0	0.0	0.0	9.1	0.0	0.0	0.0	0.0	0.0	0.0	0.0	0.0	0.0	2.06	11.41	0.0
5-16- 66	0.66	0.0	0.0	0.0	0.0	0.0	0.0	7.8	0.0	0.0	0.0	0.0	0.0	0.0	0.0	0.0	0.0	2.03	11.66	0.0
5-16- 67	0.55	0.0	0.0	0.0	0.0	0.0	0.0	6.3	0.0	0.0	0.0	0.0	0.0	0.0	0.0	0.0	0.0	1.98	11.95	0.0
5-16- 68	0.48	0.0	0.0	0.0	0.0	0.0	0.0	5.4	0.0	0.0	0.0	0.0	0.0	0.0	0.0	0.0	0.0	1.94	12.30	0.0
5-16- 69	0.39	0.0	0.0	0.0	0.0	0.0	0.0	4.1	0.0	0.0	0.0	0.0	0.0	0.0	0.0	0.0	0.0	1.84	13.23	0.0
5-16- 70	0.34	0.0	0.0	0.0	0.0	0.0	0.0	3.1	0.0	0.0	0.0	0.0	0.0	0.0	0.0	0.0	0.0	1.67	15.50	0.0
5-16- 71	16.49	0.0	0.0	0.0	0.0	0.0	0.0	204.3	0.0	0.0	0.0	0.0	0.0	0.0	0.0	0.0	0.0	2.34	10.81	0.0
5-16- 72	20.31	0.0	0.0	0.0	0.0	0.0	0.0	250.9	0.0	0.0	0.0	0.0	0.0	0.0	0.0	0.0	0.0	2.35	10.84	0.0
5-16- 73	21.81	0.0	0.0	0.0	0.0	0.0	0.0	273.9	0.0	0.0	0.0	0.0	0.0	0.0	0.0	0.0	0.0	2.36	10.65	0.0

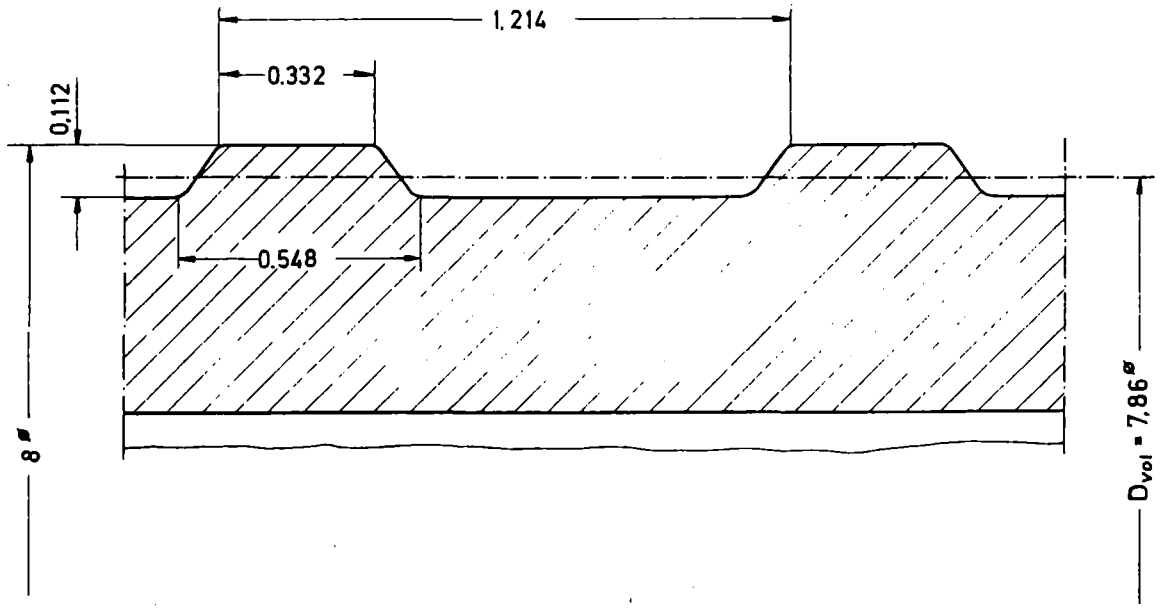

Fig.1: Roughness geometry of the present investigation

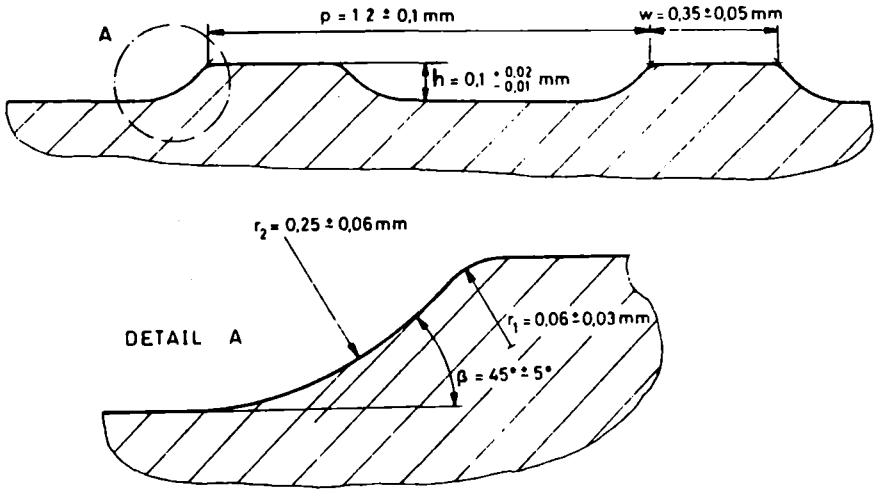

Fig.2: Roughness geometry of the EIR, KfK - joint heat transfer experiment /4/

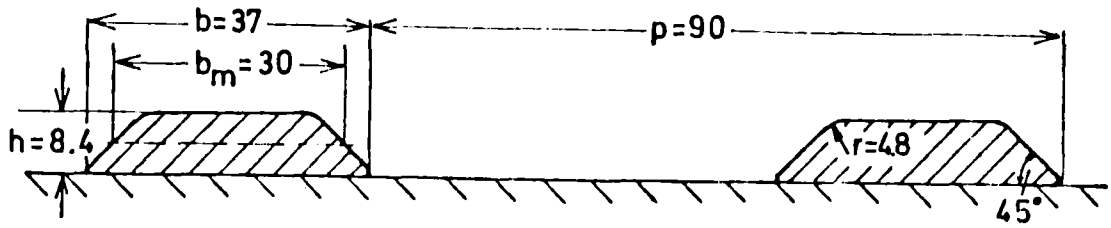

Fig.3: Roughness geometry of the investigation in the parallel plate channel /5/

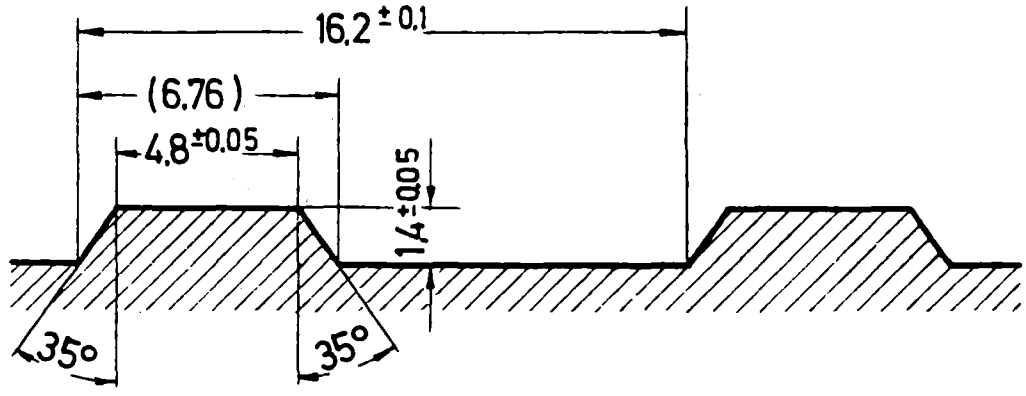

Fig.4: Roughness geometry of the investigation at a rod bundle /6/

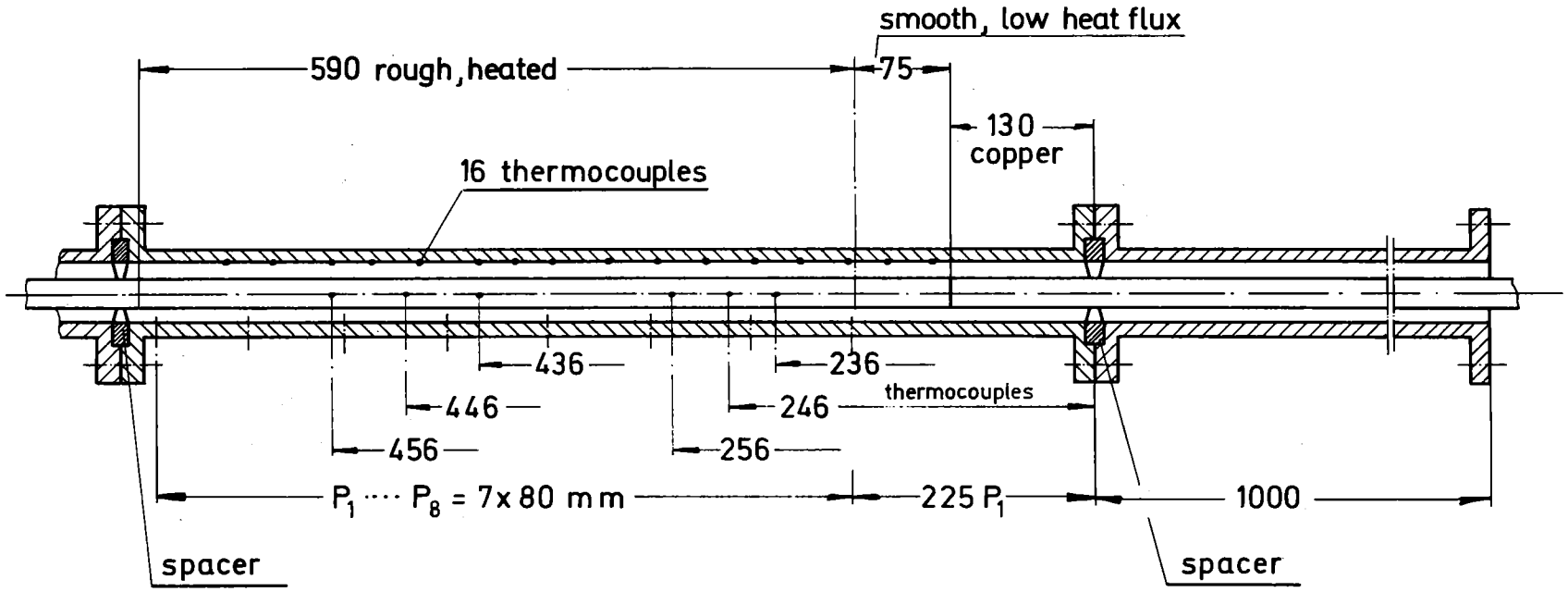

Fig.5: The test section

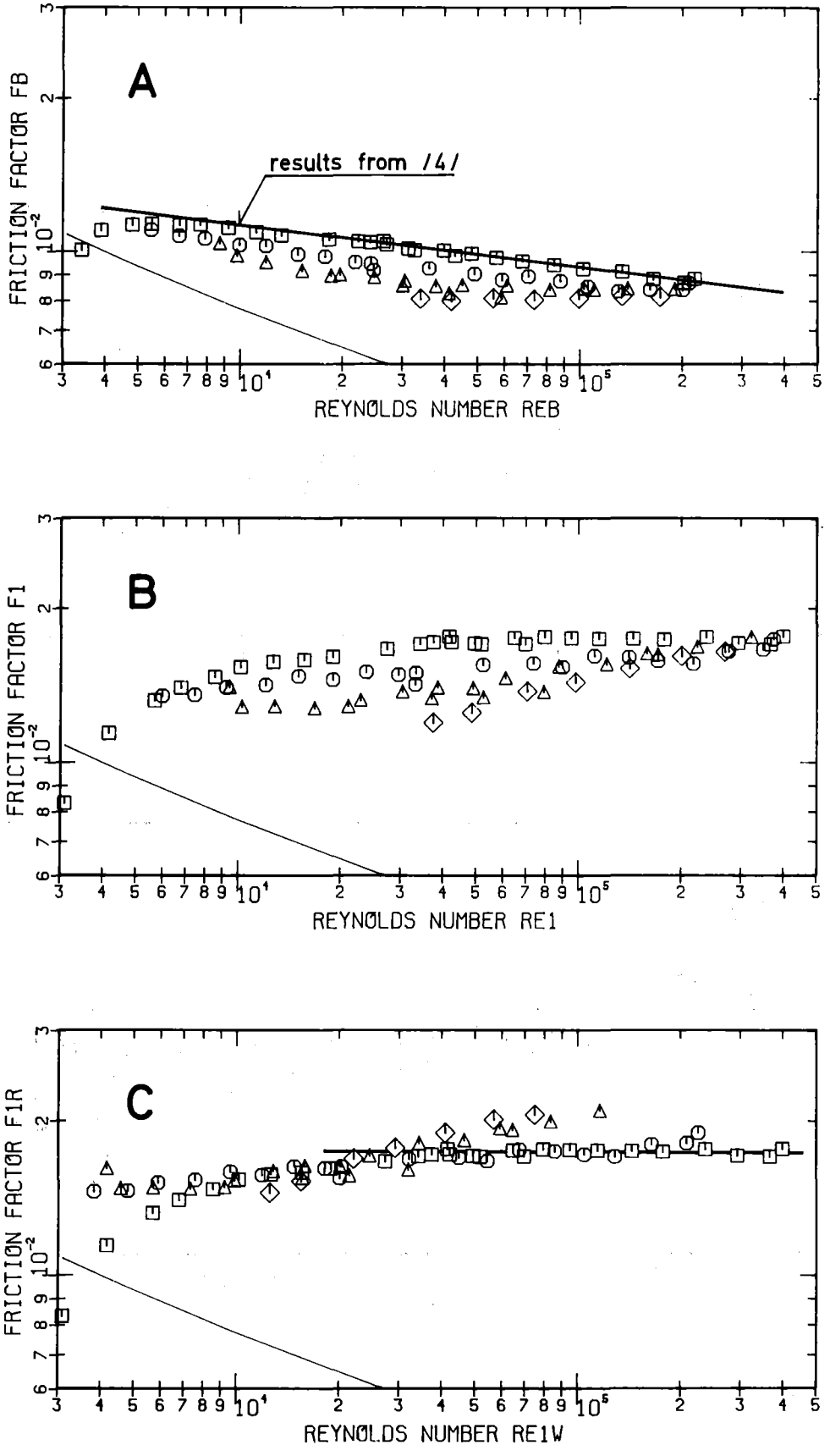

Fig.6: Friction factors versus Reynolds number

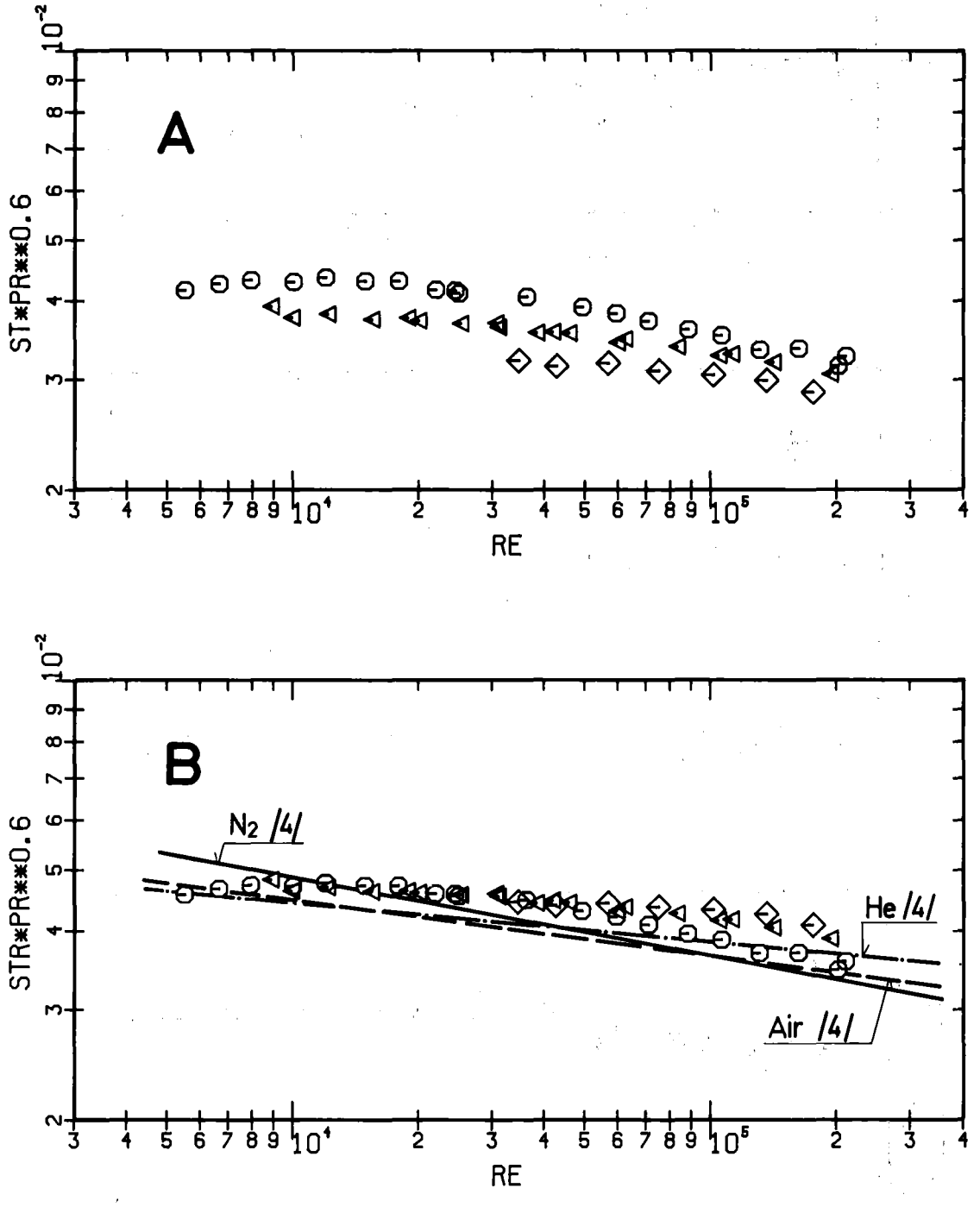

Fig.7: Stanton numbers versus Reynolds number

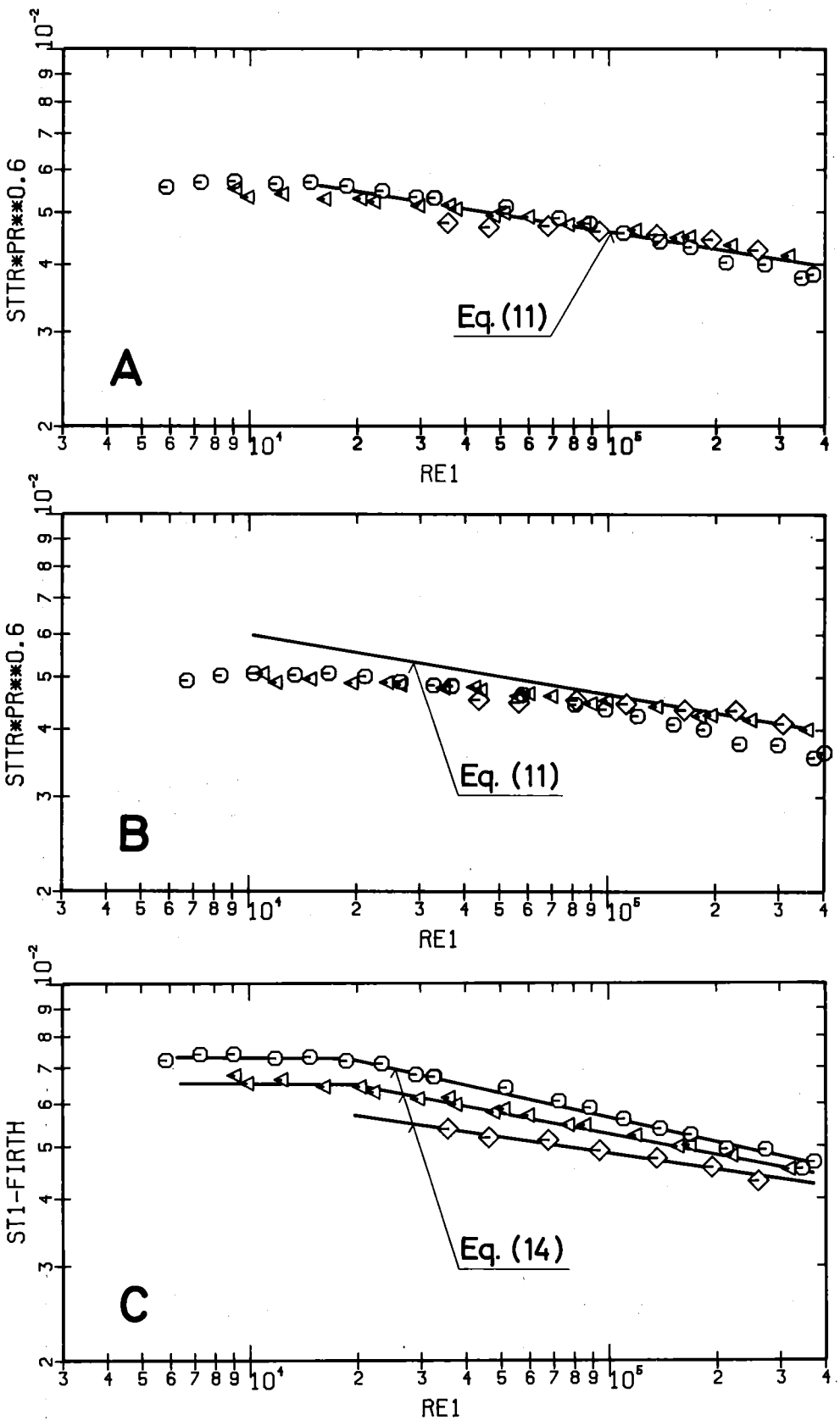

Fig.8: The transformed Stanton numbers versus Reynolds number of the rough zone
(A) transformed with A_r = 2.5
(B) transformed with A_r = 1.7
(C) transformed with Firth's method

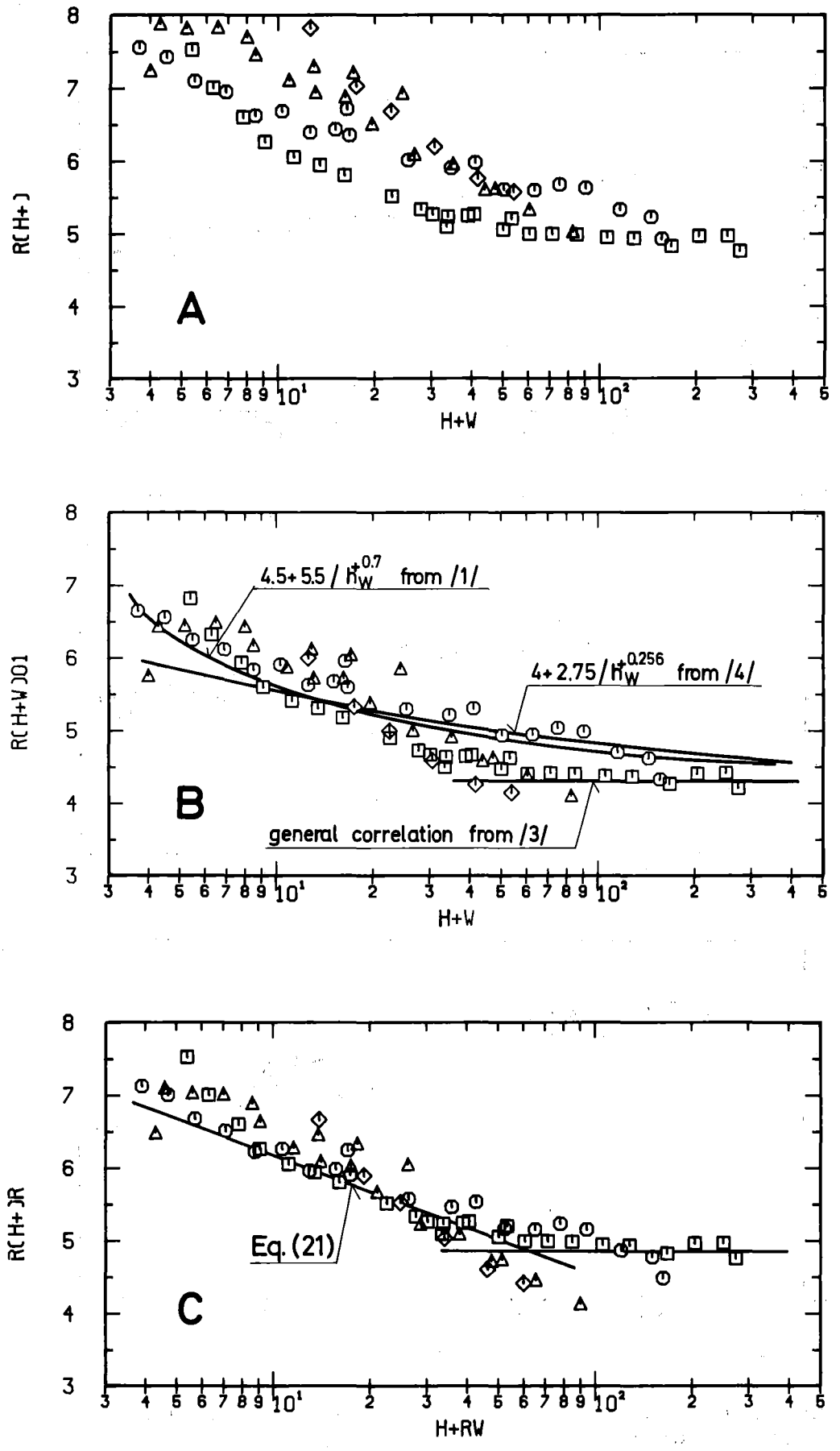

Fig.9: The roughness parameter of the velocity profile

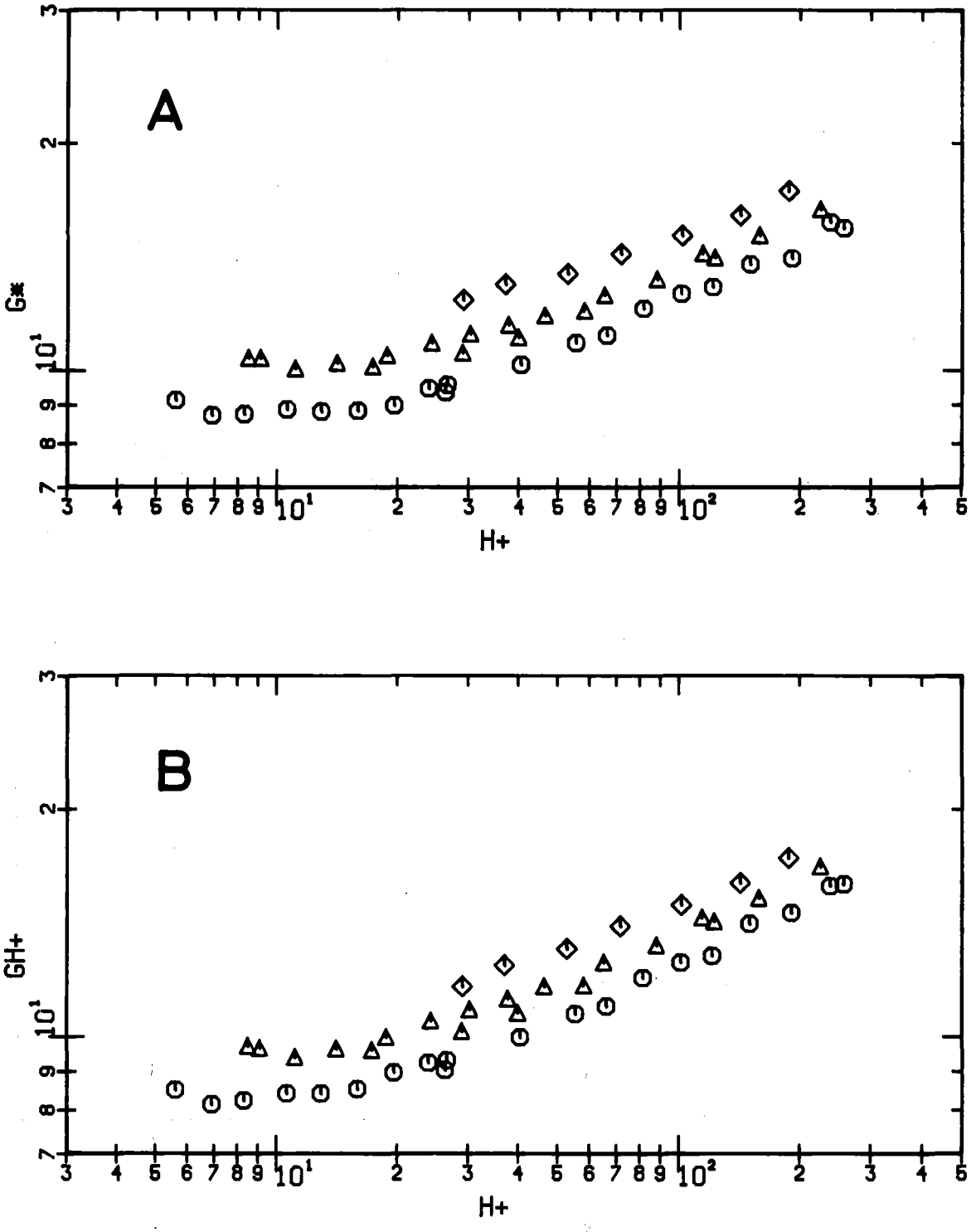

Fig.10: The roughness parameter of the temperature profile

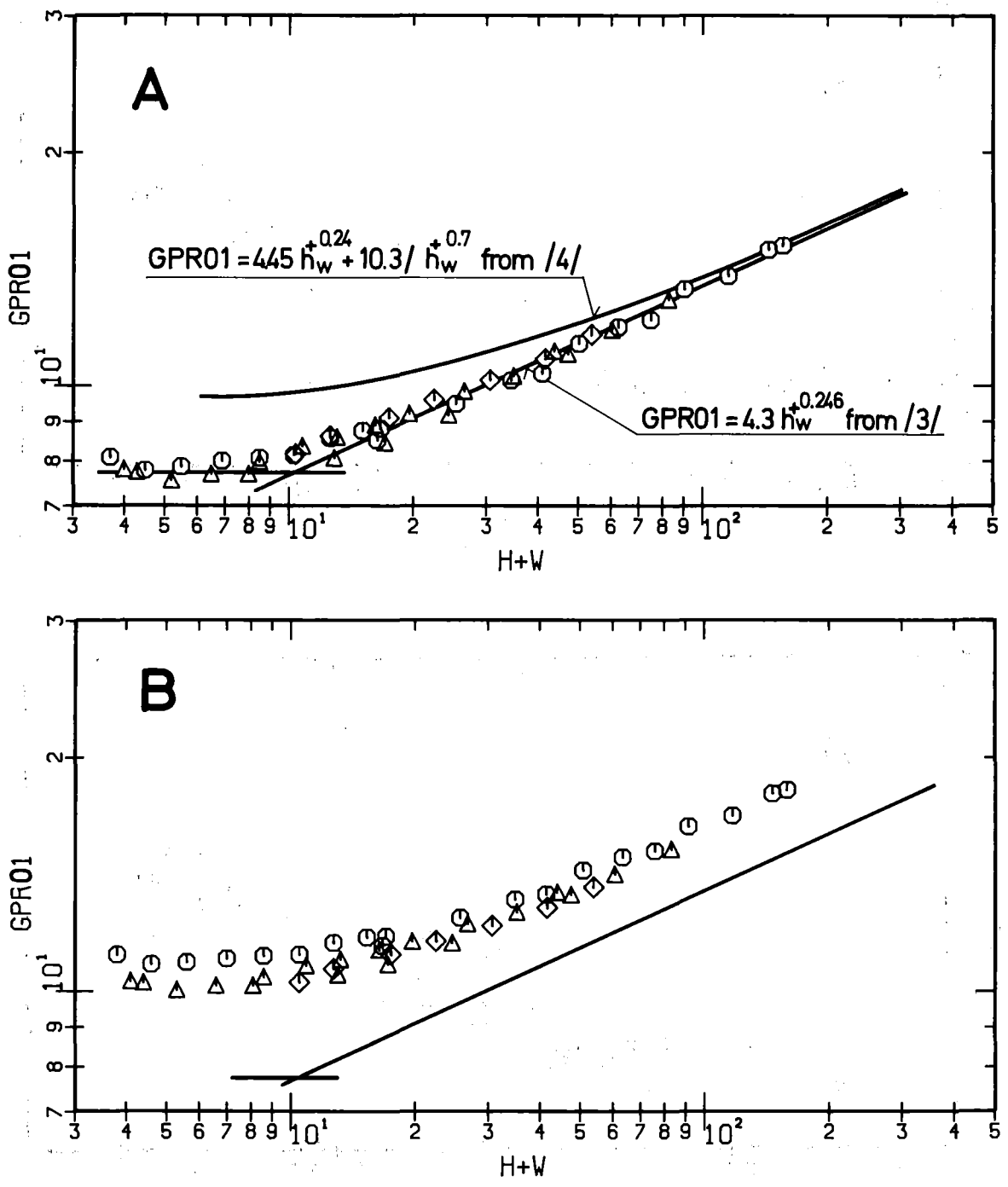

Fig.11: The reduced roughness parameter of the temperature profile (Eq.A-5) (A) evaluated with A_r = 2.5, (B) evaluated with A_r = 1.7

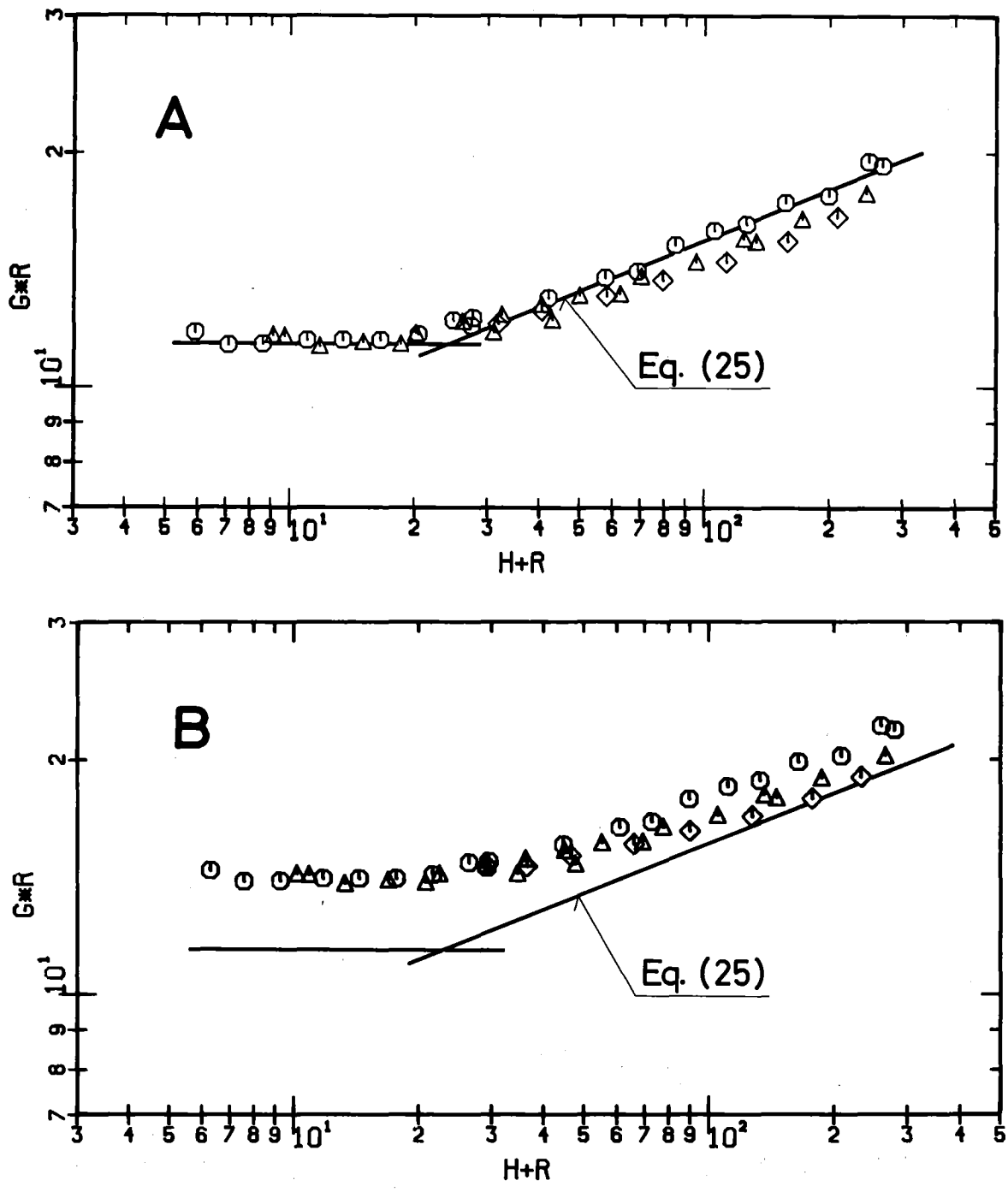

Fig.12: The reduced roughness parameter of the temperature profile (Eq.A-2) (A) evaluated with A_r = 2.5, (B) evaluated with A_r = 1.7.

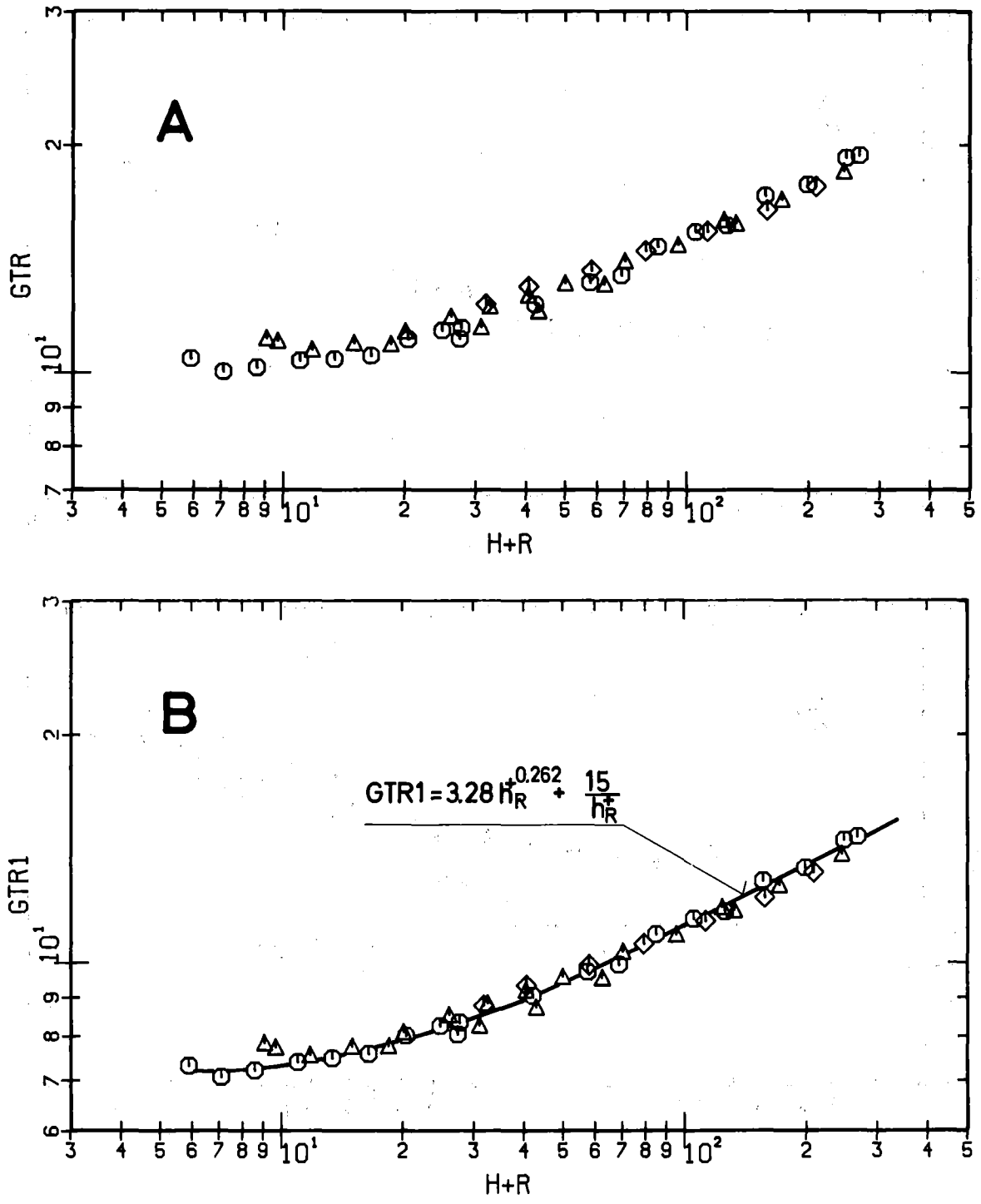

Fig.13: The transformed and reduced parameter of the temperature profile (Eqs.A-6 - A-10, A_r = 2.5).